Changes in motor unit behavior following isometric fatigue of the first dorsal interosseous muscle

Lara McManus, Xiaogang Hu, William Z. Rymer, Madeleine M. Lowery and Nina L. Suresh

J Neurophysiol 113:3186-3196, 2015. First published 11 March 2015; doi:10.1152/jn.00146.2015

J Neurophysiol 113: 3186–3196, 2015.
First published March 11, 2015; doi:10.1152/jn.00146.2015.

Changes in motor unit behavior following isometric fatigue of the first dorsal interosseous muscle

Lara McManus,[1] Xiaogang Hu,[2] William Z. Rymer,[2,3] Madeleine M. Lowery,[1] and Nina L. Suresh[2]
[1]*University College Dublin, Belfield, Dublin, Ireland;* [2]*Rehabilitation Institute of Chicago, Chicago, Illinois; and* [3]*Northwestern University, Evanston, Illinois*

Submitted 13 February 2015; accepted in final form 6 March 2015

McManus L, Hu X, Rymer WZ, Lowery MM, Suresh NL. Changes in motor unit behavior following isometric fatigue of the first dorsal interosseous muscle. *J Neurophysiol* 113: 3186–3196, 2015. First published March 11, 2015; doi:10.1152/jn.00146.2015.—The neuromuscular strategies employed to compensate for fatigue-induced muscle force deficits are not clearly understood. This study utilizes surface electromyography (sEMG) together with recordings of a population of individual motor unit action potentials (MUAPs) to investigate potential compensatory alterations in motor unit (MU) behavior immediately following a sustained fatiguing contraction and after a recovery period. EMG activity was recorded during abduction of the first dorsal interosseous in 12 subjects at 20% maximum voluntary contraction (MVC), before and directly after a 30% MVC fatiguing contraction to task failure, with additional 20% MVC contractions following a 10-min rest. The amplitude, duration and mean firing rate (MFR) of MUAPs extracted with a sEMG decomposition system were analyzed, together with sEMG root-mean-square (RMS) amplitude and median frequency (MPF). MUAP duration and amplitude increased immediately postfatigue and were correlated with changes to sEMG MPF and RMS, respectively. After 10 min, MUAP duration and sEMG MPF recovered to prefatigue values but MUAP amplitude and sEMG RMS remained elevated. MU MFR and recruitment thresholds decreased postfatigue and recovered following rest. The increase in MUAP and sEMG amplitude likely reflects recruitment of larger MUs, while recruitment compression is an additional compensatory strategy directly postfatigue. Recovery of MU MFR in parallel with MUAP duration suggests a possible role for metabolically sensitive afferents in MFR depression postfatigue. This study provides insight into fatigue-induced neuromuscular changes by examining the properties of a large population of concurrently recorded single MUs and outlines possible compensatory strategies involving alterations in MU recruitment and MFR.

motor unit action potential; surface electromyography decomposition; isometric fatigue

ADAPTATIONS IN MOTOR UNIT (MU) recruitment and firing rate modulation during contraction-induced fatigue have been proposed as compensatory mechanisms counteracting the decline in muscle force-generating capacity. The progressive recruitment of new MUs during fatiguing contractions performed at a submaximal level has been demonstrated in a number of studies, employing both sustained (Garland et al. 1994; Jensen et al. 2000; Maton and Gamet 1989) and intermittent (Adam and De Luca 2003; Bigland-Ritchie et al. 1986b; Carpentier et al. 2001; Christova and Kossev 1998; Dorfman et al. 1990; Enoka et al. 1989) fatiguing protocols. This recruitment appears to compensate for fatigue-induced loss and to aid in preserving force generation.

The role of alterations in MU firing rate and recruitment threshold in response to fatigue is less clearly defined. It has been suggested that these changes are not uniform across the MU pool (Carpentier et al. 2001; Garland et al. 1994) and that adjustments to individual MUs may depend on activation history (Farina et al. 2009). During sustained and intermittent voluntary contractions, MUs active from the beginning of the contraction typically exhibit a decline in discharge rate (Carpentier et al. 2001; Enoka et al. 1989; Garland et al. 1994); however, newly recruited MUs have been shown to exhibit a range of behaviors. Later recruited MUs have been reported to fire at a constant rate or to increase steadily (Garland et al. 1994), to exhibit no significant change in discharge rate (Adam and De Luca 2005), or to show varying rates with time (Carpentier et al. 2001). Although a decrease in the recruitment threshold of higher threshold MUs following fatigue is generally reported (Adam and De Luca 2003; Calder et al. 2008; Carpentier et al. 2001; Jensen et al. 2000), some studies have observed increased recruitment thresholds for early recruited MUs (Carpentier et al. 2001; Farina et al. 2009). Others have reported a homogenous and monotonic decrease in the recruitment threshold of their sample MU population as fatigue progressed (Adam and De Luca 2003; Christova and Kossev 1998).

A key factor that may account for the variations observed could be the type of MU recordings that are utilized. The use of surface electromyography (sEMG) is often preferred over intramuscular recordings as a more stable recording during dynamic or fatiguing contractions, with surface EMG providing a summary representation of MU behavior. Yet, to gain a comprehensive view of compensatory recruitment and firing rate strategies, it is imperative to analyze changes occurring at the MU level. These in turn can provide context from which to interpret the adaptations in the sEMG signal.

Recent advances in sEMG decomposition methods have provided a promising new method for analyzing the activity of individual MUs without the limitations associated with intramuscular EMG. A number of different sEMG configurations have been employed to date (Gazzoni et al. 2004; Hogrel 2003; Holobar et al. 2009; Kleine et al. 2008; Nawab et al. 2010). Kallenberg and Hermens (2008) observed an increase in the number of MUAPs detected per second over the course of a sustained fatiguing contraction in the biceps brachii. Although the method collectively considered both MU recruitment and firing rate, the corresponding increase in the mean root-mean-squared (RMS) amplitude of identified MUAPs suggests re-

Address for reprint requests and other correspondence: L. McManus, Univ. College Dublin, Belfield, Dublin 4, Ireland (e-mail: lara.mc-manus@ucdconnect.ie).

cruitment was the primary factor in maintaining force output. Calder et al. (2008) used a decomposition-based algorithm to identify firing times of individual MUs and extracted corresponding MUAPs by spike trigger averaging the sEMG signal from the biceps brachii. They similarly reported that increases in mean MUAP amplitude and area were mirrored by increases in the sEMG signal amplitude as the contractions progressed. This was accompanied by a significant decrease in mean MU firing rates, despite a constant torque output. A reduction in mean firing rates was also reported for MUAPs detected in the vastus lateralis, but not in the vastus medialis, in response to an intermittent fatiguing protocol (Stock et al. 2012).

It has not yet been evaluated whether a systematic approach to MU firing rate modulation and MU recruitment strategies is employed to compensate for force deficits in a fatigued muscle, due partly to the varied fatiguing protocols employed. In particular, it remains unclear whether firing rate adaptations due to fatigue are uniform across the motoneuron pool and whether there are simultaneous changes in MU recruitment strategies, such as compressed recruitment and/or recruitment of larger MUs. For technical reasons, compensatory mechanisms in a fatigued muscle have not yet been systematically assessed over a large population of concurrently recorded units.

To address these questions, the objective of our study was to compare MU behavior directly after isometric fatigue, and following partial recovery, to prefatigue conditions in the first dorsal interosseous (FDI) muscle. The aim of this approach is to comprehensively assess the relative contribution of MU firing rate and recruitment strategies in accommodating for muscle force impairment in a fatigued hand muscle. In addition, the ability to record a large sample MU population using a sEMG decomposition system (dEMG) allows us to determine the degree of uniformity of these adaptations across the MU pool.

This study characterizes the response of a population of MUs following isometric fatigue using a dEMG system that utilizes a novel surface sensor array recording electrode, coupled with advanced pattern recognition software to identify single MUAPs. The dEMG approach has been validated with a range of different techniques (De Luca and Nawab 2011; Hu et al. 2013a,b), using a two-source recording method (Hu et al. 2014), as well as several advanced simulation studies. It has been used to investigate the control of multiple MUs in voluntary contractions in intact subjects (De Luca and Hostage 2010; Defreitas et al. 2014), during fatigue (Beck et al. 2012; Stock et al. 2012), and in stroke survivors (Hu et al. 2012). The dEMG system allows MU behavior in a fatigued muscle to be characterized using both the standard sEMG signal and information from individual MUAPs. The relationship between the two recordings can also be examined to determine which MU properties predominate in mediating the changes in the sEMG signal.

Our results show an increase in sEMG and MUAP amplitude postfatigue and following a recovery period, indicating the recruitment of larger MUs to compensate for the decline in the force-generating capacity of the fatigued muscle. MUAP duration increased directly postfatigue but recovered after the rest period, suggesting the restoration of the ionic and metabolic changes to the muscle that slow muscle fiber conduction velocity (MFCV). This was accompanied by a parallel decrease and subsequent increase in MU firing rates, consistent across the MU pool. The reduction in firing rates coupled with continued recruitment may suggest a selective inhibition of early recruited motoneurons, mediated through increased activity of mechanically and metabolically sensitive afferents. The results indicate that a combination of supplementary MU activation and lower MU recruitment threshold is favored over rate coding to maintain the force after fatigue while MUs are available.

METHODS

Participants. Twelve right-dominant neurologically intact individuals (6 male, 6 female) volunteered to participate in this study. The force and EMG activity of the first dorsal interosseous muscle were examined during isometric abduction of the right index finger about the second metacarpo-phalangeal (MCP) joint. All participants gave informed consent via protocols approved by the Institutional Review Board under the Office for the Protection of Human Subjects at Northwestern University.

Experimental setup. Participants were seated upright in a Biodex experimental chair (Biodex Medical Systems, Shirley, NY) with their upper arm comfortably resting on a plastic support. To standardize hand position and to minimize contributions of unrecorded muscles, the forearm was cast and placed in a ring mount interface attached to an elbow rest at the wrist. The elbow rest was securely mounted with magnetic stands to a heavy steel table. The forearm was placed in full pronation and the wrist was held neutral with respect to flexion/extension. The little, ring, and middle fingers were separated from the index finger and strapped to the support surface. The thumb was secured at an ~60° angle to the index finger. The index finger was placed in line with the second metacarpal and the long axis of the forearm creating a 0° or neutral (abduction/adduction) MCP joint angle. The proximal phalanx of the index finger was fixed to a ring-mount interface attached to a six degrees-of-freedom load cell (3226; ATI). Recorded forces from the x (abduction/adduction)- and y (extension/flexion)- directions were low pass filtered (cut-off = 200 Hz) and digitized at a sampling frequency of 1 kHz. The subjects were instructed to produce required abduction forces while minimizing the off-axis forces. There is evidence that both MU recruitment threshold (Enoka et al. 1989) and patterns of recruitment (Suresh et al. 2002) are directionally dependent (i.e., finger flexion vs. abduction) in the FDI. To prevent variations in rank order of MU recruitment with different directions of contraction (Thomas et al. 2006) off-axis forces in the flexion direction were tightly controlled. The subject received visual feedback of the force in the x and y direction (flexion/extension) to minimize off axis forces and maximize the force exerted in the desired x direction.

The subject's skin was prepared using adhesive tape and alcohol pads. sEMG was recorded from the FDI using a surface sensor array (Delsys) that consisted of five cylindrical probes (0.5-mm diameter) located at the corners and at the center of a 5 × 5 mm square (Nawab et al. 2010). Pairwise differentiation of the five electrodes yielded four channels of sEMG signals (Fig. 1*A*). The sEMG sensor and a reference electrode were connected to four channels of a Bagnoli sEMG system (Delsy). The signals were amplified and filtered between 20 Hz and 2 kHz. The signals were sampled at 20 kHz and stored on a computer for further processing.

Protocol. Subjects were asked to perform a series of three maximal voluntary contractions (MVCs) for 3 s, with a 1-min rest between trials, and the largest value was designated as 100% MVC. The subjects were then asked to perform a series of six isometric voluntary contractions in which they followed a trapezoidal force trajectory as depicted in Fig. 1*B* to provide a prefatigue baseline. Feedback on the force direction and magnitude was presented to the subject in two-dimensional display on a computer screen as a visual aid. The

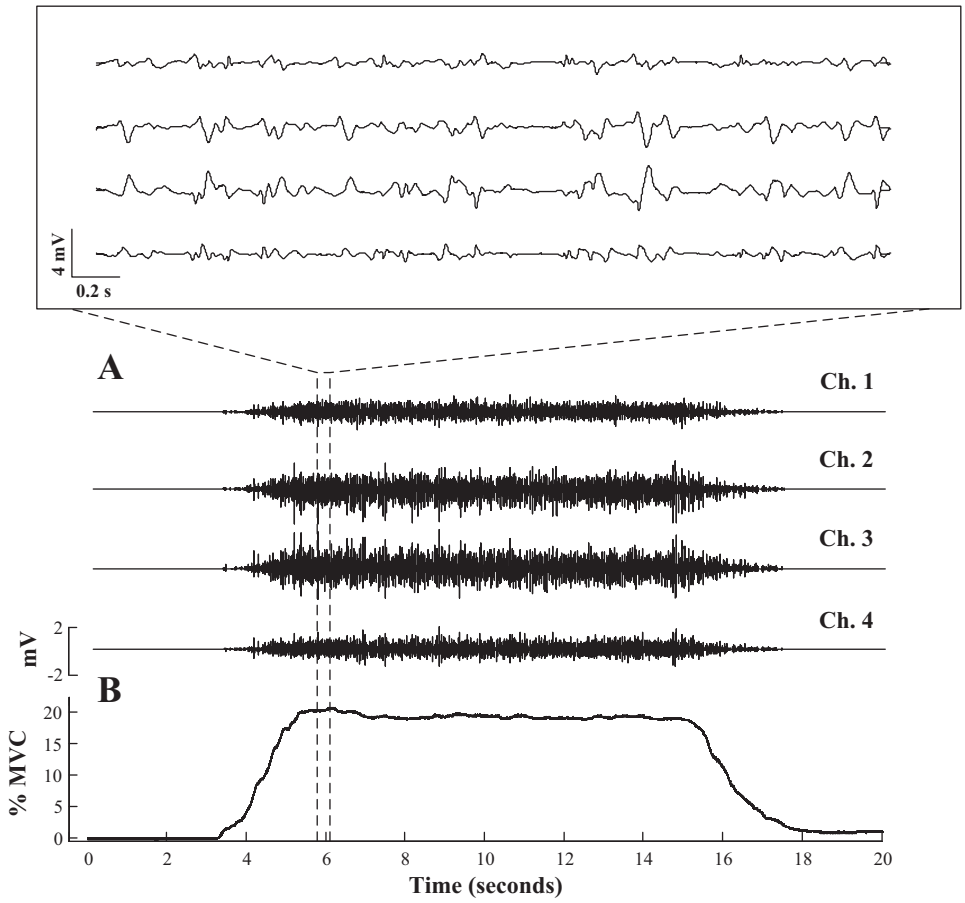

Fig. 1. Four channels of surface electromyography (sEMG; *A*) recorded from the 1st dorsal interosseous (FDI) using the precision decomposition system during a 20-s 20% maximum voluntary contraction (MVC) trapezoidal force trajectory (*B*).

dimensions of the target on screen were kept constant across subjects; therefore, visual gain was maintained over the experiment for a single subject but varied between subjects according to subject MVC. Previous studies have indicated that alterations to visual gain can influence force fluctuations (Sosnoff and Newell 2009) and motoneuronal excitability (Laine et al. 2014). However, in this study intersubject differences in visual feedback were relatively small and were unlikely to have had significant effects on force variability (Baweja et al. 2009). The trapezoid trajectory contained five segments: a 3-s quiescent period for baseline noise calculation, an up-ramp increasing at a rate of 10% MVC/s, a constant force of 20% MVC for 10 s, a down-ramp decreasing at 10% MVC/s, and a final 3-s quiescent period. To ensure that the subjects could trace the trapezoid trajectory closely, they were given practice trials before the main experiment. During this section of the experiment, the subject was given a 1-min rest period between repetitions to minimize fatigue. After the six prefatigue trials, a sustained isometric contraction was performed at 30% MVC to task failure to induce fatigue. The subjects were given visual bar feedback of their force output, and the time of task failure was defined as the time when the subject's force dropped 10% below the required output for a period of 5 or more seconds. A single MVC was performed directly following task failure, and six postfatigue trapezoidal force trajectories at 20% MVC were subsequently performed, with no rest period given between trials to minimize recovery. The subjects were then allowed a 10-min recovery period before a series of four more trapezoidal trajectories (20% MVC) was performed. A final MVC was recorded in 10 of the subjects following the recovery trials.

Data analysis. To be selected for further analysis, sEMG signals were required to have a peak to peak (P-P) baseline noise <20 μV and signal to noise ratio >5 with no sudden change (i.e., $l > 20\%$ MVC/s) in the up-ramp force. The analysis was confined to the sEMG signals recorded before and directly after the fatiguing contraction, and following the recovery period, to adhere to specific experimental conditions for which the dEMG system has been previously validated, i.e., short duration isometric contractions. Next, discriminable MUs were extracted using the dEMG decomposition system (version 1.0.0.28). For each identified MU, the output of the algorithm consisted of MU firing times and four MUAP waveforms (for the 4 recorded channels). Detailed information for the decomposition algorithms is described in Nawab et al. (2010) and De Luca and Hostage (2010).

Spike-triggered averaging (STA) of the sEMG was performed to characterize the MU waveform recorded from the surface electrodes. A STA was performed on each of the four channels of the sEMG signals, using the identified firing times for each MU as triggers, resulting in four representative STA MUAP estimates for each MU. The time interval used to derive the template estimate was 10 ms before and after the firing time. The peak-to-peak amplitude was calculated as the voltage difference between the maximum peak and the adjacent minimum peak within the time window. The time between the nearest zero crossings to the maximum and minimum peaks was calculated to provide the MUAP duration.

Two separate reliability tests were performed to determine which decomposed MUAP estimates would be retained for further analysis, using the procedure outlined in Hu et al. (2013b). To quantify the variation of the STA MUAP over time, the coefficient of variation (CV) was calculated for the P-P amplitude of the MUAP templates. This coefficient was implemented as a measure of the stability of the waveform average over the duration of the contraction and the accuracy of the firing time estimation. The maximum linear correlation coefficient between the STA estimate (calculated over the entire trial duration) and the decomposition-estimated templates was computed as a second measure of the reliability of the STA estimates of

the MUAP. The MUs with an average correlation coefficient (between the STA MUAP estimate and the decomposition MU template) >0.7 and CV of P-P amplitude <0.3 across all four channels were selected for further analysis. For each identified MU, the combined results from all four channels was used only for the MU selection process, subsequent analysis of the selected MUs was simplified by using the channel of maximum median amplitude for each subject.

The recruitment threshold was defined as the threshold force at recruitment, calculated as the averaged force over the interval −50 to +100 ms relative to the first firing event. The mean firing rate was calculated with a nonoverlapping window of a 0.5-s length from a 4-s averaging window in the middle of the steady-state hold phase of the contraction. The relationship between the MUAP amplitude/duration and the recruitment threshold force of the MU was examined by fitting a linear regression line to the data and calculating the slope and r squared values of the fit.

To assess the relationship between spectral properties of the global signal and characteristics of the decomposed MUAPs, the mean RMS and the median frequency of the power spectrum (MPF) value of the sEMG signal during the trapezoidal force trajectories were calculated for each subject for each of the three conditions (pre- and postfatigue and recovery). The average values were obtained using a 1-s moving average window and step size of 0.5 s over 2 s of the steady-state hold phase (7–9 s) using the first trial at 20% MVC.

The RMS value of the EMG signal was calculated across a 1-s time window (5–6 s) during the 30% MVC fatiguing contraction for each subject. To control for between-subject variations in sEMG amplitude, this RMS value was used to normalize the RMS amplitude of the global signal detected for each condition. The mean and SD of the decomposed MUAP amplitudes were calculated for the MUs detected in the prefatigue condition for each subject and used to standardize the prefatigue MUAP amplitude distribution to have a zero mean and unit variance. The prefatigue mean and SD were then used to standardize the postfatigue and recovery MUAP distributions within the same subject. Standardized distributions were used to examine the changes in MUAP amplitude with condition across subjects and reduce subject specific variability in the mean and variance of the distribution.

Statistics. For each subject, the median value of the MPF and RMS of the global sEMG signal and the amplitude and duration of the surface decomposed MUAPs were calculated for the prefatigue, postfatigue, and recovery states. The probability distributions of the decomposed MUAP amplitudes and durations were analyzed per condition for each subject. A one-way within-subjects (or repeated measure) ANOVA was conducted to compare the effect of condition on each parameter across subjects, with a statistic test for prefatigue, postfatigue, and recovery states. Mauchly's test of sphericity was implemented to check the assumption of sphericity, and if violated, a Greenhouse-Geisser correction was applied to the data. Post hoc tests to examine pairwise differences between conditions were conducted using the Fisher's least significant difference test. A regression analysis using a generalized linear model was performed to examine the change of MPF and RMS of sEMG during the fatigue protocol.

RESULTS

The properties of the sEMG signal and the characteristics of multiple discriminated MU spike trains, including mean firing rates and the estimated threshold force, were examined before and after a fatiguing contraction. The alterations in median MUAP amplitude and duration were related to the changes observed in the RMS amplitude and mean frequency of the surface signal. Changes in MUAP amplitude and duration and MU firing rate were examined as a function of MU recruitment threshold to assess the uniformity of the adaptations across the MU pool.

Force properties. Changes in subject MVC across the conditions (for $n = 10$ subjects) were analyzed with an ANOVA before and after the sustained isometric 30% MVC fatiguing contraction to task failure (196.8 ± 55 s). The results indicate a significant difference in subject MVC between pre- and postfatigue conditions [$F(2,18) = 33.895$, $P < 0.0001$]. Post hoc tests revealed a significant reduction ($P < 0.001$) in MVC following fatigue (54.15 ± 11.53 to 30.43 ± 13.36 N, respectively). The median subject MVC failed to recover after the period of rest and remained significantly depressed (42.75 ± 16.75 N, $P < 0.001$) compared with initial prefatigue values, though higher than that recorded directly postfatigue ($P < 0.005$).

sEMG signal. The results of an ANOVA, with Greenhouse-Geisser correction, show that there was a significant effect of condition (prefatigue, postfatigue, and recovery) on the EMG MPF [$F(1.18,12.99) = 20.123$, $P < 0.0001$; Fig. 2*A*]. Post hoc tests revealed that the sustained, fatiguing contraction resulted in a significant decrease in global signal MPF from prefatigue to postfatigue conditions (166.9 ± 52.09 to 100.38 ± 31.42 Hz, respectively, $P < 0.001$, standardized values 0 ± 1 to −1.27 ± 0.6). However, after the recovery period the MPF increased significantly (170.87 ± 79.04 Hz, $P = 0.002$, standardized value 0.08 ± 1.5) and was found not to be statistically different from MPF values before fatigue ($P = 0.709$).

ANOVA on the mean scores for normalized RMS amplitudes also confirmed a significant effect of condition [$F(2,22) = 7.08$, $P = 0.004$; Fig. 2*B*]. Median normalized RMS amplitude increased significantly ($P = 0.023$) from prefatigue to postfatigue conditions (1.01 ± 0.075 to 1.36 ± 0.47 and 0.19 ± 0.18 to 0.26 ± 0.14, normalized and nonnormalized values, respectively). After the period of 10-min recovery mean RMS am-

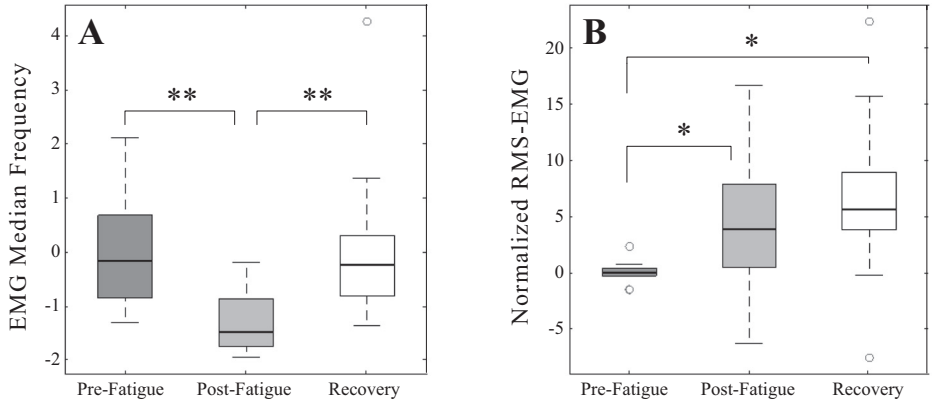

Fig. 2. Median values for median power frequency (*A*) and root-mean-squared (RMS; *B*) amplitude of the global sEMG signal across all subjects for prefatigue, postfatigue, and recovery conditions. Median values were calculated from data recorded during the steady-state hold (7–9 s) of the trapezoidal force trajectory. All values were standardized to the mean and SD of prefatigue values. *$P < 0.05$ and **$P < 0.005$, significant differences.

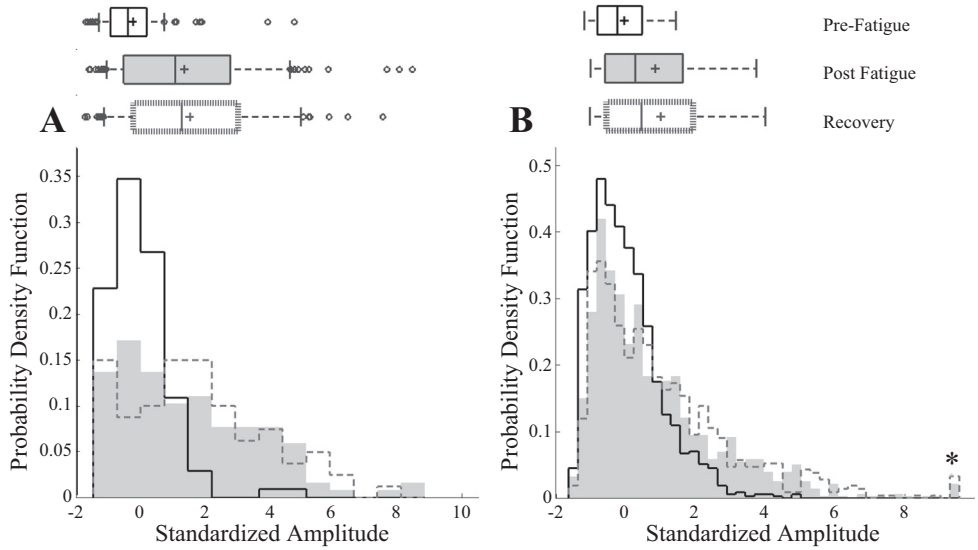

Fig. 3. Probability distribution of motor unit (MU) amplitudes (a) for a single subject (*A*) and across all subjects (*B*). Boxplots display the mean (line), median ("+"), SD, and outliers of the distribution. MU amplitudes for each subject have been standardized to his or her prefatigue values for comparison. *Postfatigue and recovery conditions 6 and 7 MUAP amplitudes, respectively, were >9.26.

plitude (1.49 ± 0.56, normalized, 0.29 ± 0.13, nonnormalized) remained elevated with respect to the initial RMS mean ($P = 0.012$); however, the values were not significantly different to postfatigue values ($P = 0.198$).

Decomposed MUAPs. Within each condition prefatigue, postfatigue, and after the recovery period, 78.6% (1164 of 1480 MUs), 76% (1052 of 1384 MUs), and 78% (784 of 1001 MUs) were accepted, respectively. Unless otherwise stated the values reported are based on the analysis of accepted units. Over all conditions, 77% of decomposed MUs met the criteria to be accepted for further analysis. The probability density distribution in Fig. 3 displays the probability of occurrence of an accepted MU of a particular amplitude plotted against increasing amplitude values in a single representative subject and across all subjects for prefatigue, postfatigue, and after a 10-min recovery. Boxplots display the mean (line), median ("+"), SD, and outliers of the distribution for the indicated MU population. Figure 4 shows the corresponding probability distribution of the MU durations in a single representative subject and across all subjects.

Repeated-measures ANOVAs were then employed to examine the intrinsic signal properties of the decomposed MUAPs. The change in MVC (Fig. 5*A*) was accompanied by a significant change in the duration of the decomposed MUAPs with condition [$F(2,22) = 79.97$, $P < 0.0001$; Fig. 5*B*]. Median MU duration increased significantly ($P < 0.0001$) from prefatigue to postfatigue conditions (7.05 ± 1.29 vs. 10.21 ± 2.03 ms, respectively). However, after the recovery period median MU durations then decreased significantly (7.26 ± 1.74 ms, $P < 0.0001$) and were found not to be statistically different from durations observed before fatigue ($P = 0.329$).

The results of an repeated-measures ANOVA, with Greenhouse-Geisser correction, on the median standardized amplitudes of decomposed MUs reveal that the median MUAP amplitude was significantly affected by fatigue [$F(1.3, 14.3) = 7.57$, $P = 0.01$; Fig. 5*C*]. An increase in median standardized MU amplitude was observed from prefatigue to postfatigue conditions (−0.2 ± 0.058 vs. 0.46 ± .97, respectively), which was statistically significant ($P < 0.05$). However, after the period of 10 min recovery MUAP amplitudes (0.7 ± 0.99) remained significantly higher than prefatigue values ($P < 0.01$). No statistical difference was observed between the medians of the two sets of MUAP amplitudes recorded after the fatiguing contraction, whether recorded directly after or following the recovery period ($P = 0.068$).

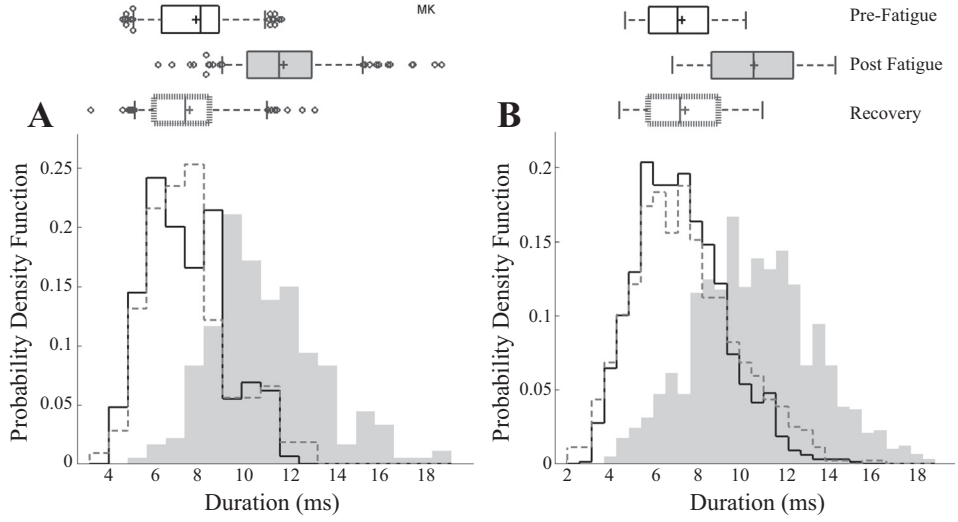

Fig. 4. Probability distribution of MU durations for a single subject (*A*) and across all subjects (*B*). Boxplots display the mean (line), median ("+"), SD, and outliers of the distribution.

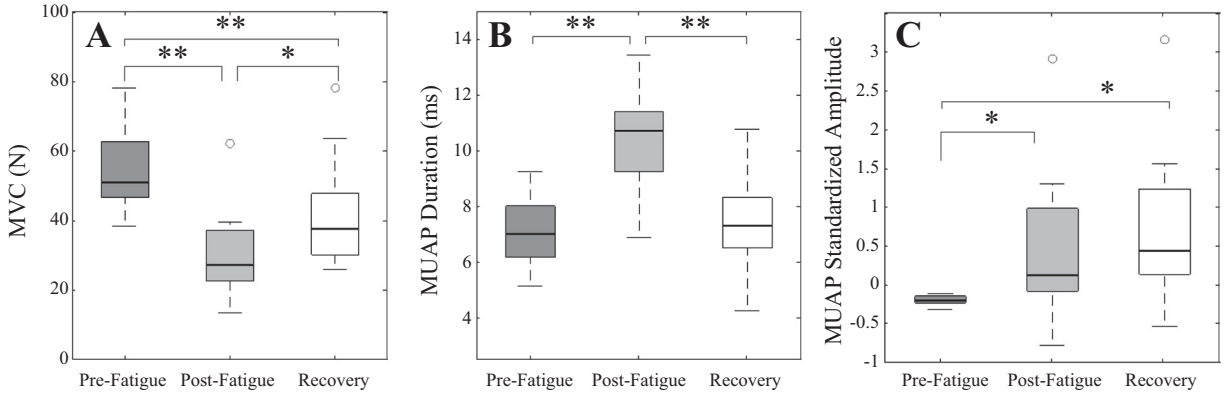

Fig. 5. Maximum voluntary contraction (*A*), median MUAP duration (*B*), and median standardized MUAP amplitude (*C*) for the decomposed MUAPs across all subjects for prefatigue, postfatigue and recovery conditions. *$P < 0.05$ and **$P < 0.001$, significant differences.

To investigate whether there was any systematic bias in the method employed to retain MUs for further analysis, the ANOVAs were repeated using all of the original decomposed MUs. There was no difference in the direction of any of changes in MU amplitude or duration for each condition.

MU firing rate changes. Repeated-measures ANOVAs were then employed to examine the mean firing rates over each condition. The results show that there was a significant effect of condition on the firing rates of the decomposed MUAPs [$F(2,22) = 10.04$, $P < 0.001$; Fig. 6*B*]. Median MU mean firing rate decreased significantly ($P < 0.015$) from prefatigue to postfatigue conditions (10.9 ± 1.26 vs. 10.15 ± 1.47 Hz, respectively). However, after the recovery period median MU firing rates then increased significantly (11.23 ± 1.27 Hz, $P < 0.001$) and were found not to be statistically different from discharge rates observed before fatigue ($P = 0.218$).

The average firing rate of MUs was calculated within a bin width equal to 1% MVC for each subject over all conditions and the mean result for all subjects is displayed in Fig. 6*B*. A significant negative correlation was observed between threshold of recruitment and average firing rates per bin for prefatigue, postfatigue, and recovery conditions [$r(101) = -0.7$, $P < 0.001$; $r(85) = -0.6$, $P < 0.001$; and $r(103) = -0.73$, $P < 0.001$, respectively].

MU recruitment threshold. Figure 7 presents the probability distribution of the recruitment threshold for the MUAP pool. The results of a repeated-measures ANOVA show a significant effect of condition on the median threshold of recruitment for decomposed MUAPs [$F(2,22) = 3.497$, $P < 0.05$; Fig. 7]. Median MU threshold of recruitment was significantly lower directly post fatigue (5.75 ± 2.06% MVC) than both prefatigue and recovery conditions (7.83 ± 2.96% MVC, $P < 0.05$, and 7.89 ± 3.09% MVC, $P < 0.05$, respectively).

The normalized MUAP amplitude for each subject was binned with respect to its threshold of recruitment with a bin width of the normalized force equal to 1% MVC. The average MUAP amplitude in the postfatigue and recovery conditions was greater than the corresponding prefatigue average at each threshold bin; however, there was no consistent trend to suggest that lower or higher threshold MUs were affected disproportionately. Similarly, the increase in the average duration of MUAPs detected at each 1% MVC force interval after fatigue did not appear to be influenced by the initial MU recruitment threshold.

Effect of recruitment threshold on measured parameters. The uniformity of MUAP property changes across the MU pool was investigated by examining the relationship between the decomposed MUAP amplitude/duration and the recruitment threshold force of the MU. No correlation was observed between MUAP duration and recruitment threshold force; the linear regression slope did not differ significantly from zero for 96% of the trials. We found no systematic change with condition for either the slope or the *r*-squared value of the linear regression fit to the MUAP amplitude vs. threshold plot when analyzed with a repeated-measures ANOVA [$F(2,22) = 2.62$, $P = 0.095$ and $F(2,22) = 0.076$, $P = 0.927$ respectively]. This may indicate compensatory strategies postfatigue are subject specific, with a combination of recruitment compression (in-

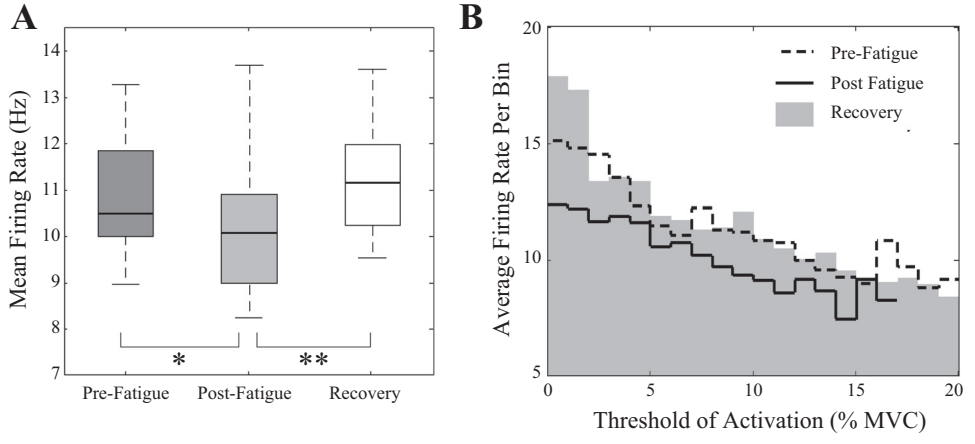

Fig. 6. Distribution of mean MU firing rates across all subjects for prefatigue, postfatigue, and recovery conditions (*A*) and average firing rate (*B*) of MUs binned with respect to the MU threshold of recruitment for all subjects. *$P < 0.05$ and **$P < 0.001$, significant differences.

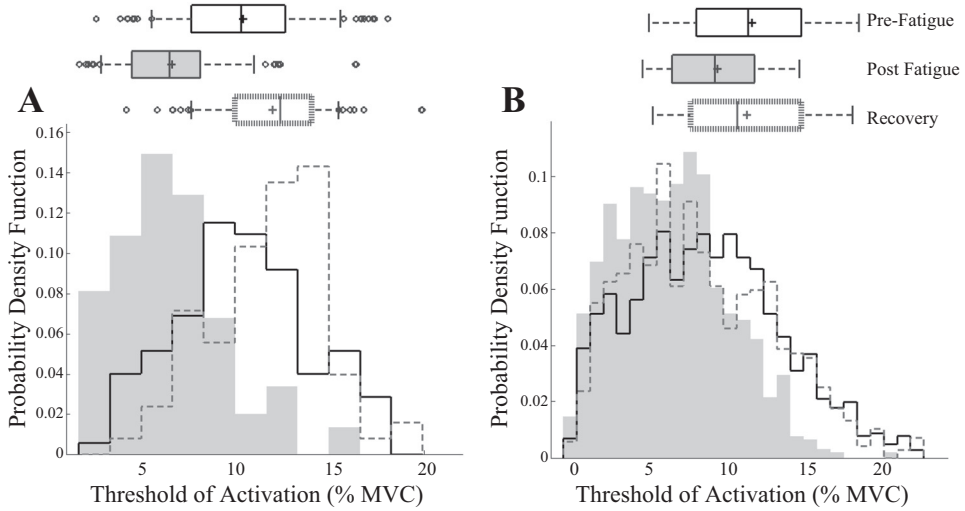

Fig. 7. Probability distribution of MU recruitment thresholds for a single subject (*A*) and across all subjects (*B*). Boxplots display the mean (line), median ("+"), SD, and outliers of the distribution.

creased slopes) and supplementary MU recruitment (no change in slope values) employed. A significant increase in amplitude with threshold was observed in only 47% of trials, which may occur as a result of the low force of the contraction. Although no consistent change in the slope of the MUAP amplitude vs. threshold plot was observed, higher mean slopes were reported directly postfatigue (0.057 ± 0.07) and after recovery (0.039 ± 0.035), than the slopes observed prefatigue (0.029 ± 0.036). In contrast, similar mean *r*-squared values were reported for all three conditions (0.32 ± 0.26, 0.33 ± 0.2, and 0.32 ± 0.2; prefatigue, postfatigue, and after recovery, respectively).

Covariation of global sEMG measures and MU parameters. An approximately linear relationship was observed between the median amplitude of decomposed MUAPs and the RMS amplitude of the global sEMG signal. The scatterplot in Fig. 8*A* presents the relationship between MUAP amplitude and sEMG amplitude for all of the three conditions, along with the Pearson product-moment correlation coefficient. A strong, statistically significant positive correlation was observed between MUAP amplitude and the amplitude of the sEMG signal [$r(36) = 0.86$, $P < 0.0001$]. A Spearman's rank-order nonparametric correlation was performed to determine the nonlinear but monotonic relationship between the median duration of decomposed MUAPs and the MPF of the global sEMG signal across each of the three conditions. The scatterplot in Fig. 8 summarizes the results; a strong, statistically significant negative correlation was observed between MUAP duration and the median frequency of the global signal [$r(36) = -0.95$, $P < .0001$].

The square of the Pearson product-moment correlation coefficient was computed to assess the approximately linear relationship between the median amplitude and firing rate of decomposed MUAPs and the percentage change between conditions for the median duration and firing rate of decomposed MUAPs. A strong, statistically significant negative correlation was observed between MUAP amplitude and firing rate [$r(36) = -0.4$, $P < 0.05$] and percentage change between conditions for MUAP duration and discharge rate [$r(36) = -0.726$, $P < 0.0001$].

DISCUSSION

In this study, sEMG and MUAP properties, including MU recruitment and firing rates, were examined collectively to provide insight into changes due to isometric muscle fatigue and in the following recovery period. While many of these techniques are well established, the capacity to decompose the sEMG signal into constituent MUAPs offers a unique overview of the distribution of MUAP waveform characteristics across a large population of MUs, an approach that has been difficult to implement using traditional surface or intramuscular EMG methods to date. The sEMG decomposition technique also allows a comprehensive, simultaneous analysis of firing rate and recruitment properties across the motor neuron pool, in a manner not previously attainable.

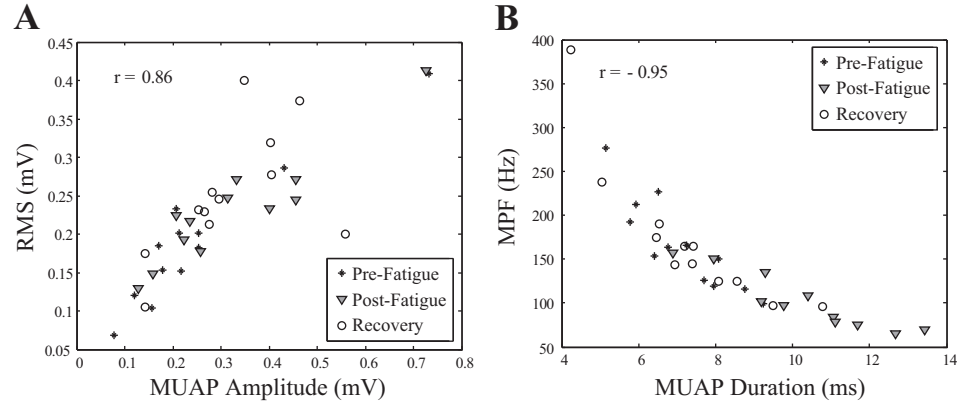

Fig. 8. Scatterplot of the median decomposed MUAP amplitude and the RMS amplitude of the global sEMG signal for all subjects for each of the 3 conditions $r = 0.86$ (*A*) and the median decomposed MUAP duration and the median frequency of the power spectrum (MPF) of the global sEMG signal for all subjects for each of the 3 conditions $r = -0.95$ (*B*).

Changes to the global EMG signal. For each subject, a sustained, fatiguing contraction induced a reduction in the force-generating capacity of the FDI muscle immediately following the contraction. The reduction in maximal force persisted beyond the 10-min recovery period (Fig. 5*A*). This incomplete recovery of force following a rest period has also been reported previously in the biceps brachii and the FDI muscles, using a similar sustained, submaximal fatiguing protocol (Esposito et al. 1998; Fuglevand et al. 1993b; Post et al. 2008). The presence of muscle fatigue is supported by a significant progressive decrease in the median frequency of the EMG signal during the sustained fatiguing contraction and immediately postfatigue (Fig. 2*A*). This is consistent with the well-established decline in muscle fiber conduction velocity as fatigue progresses. The sEMG spectral properties recorded immediately after the fatiguing contraction suggest a change in the metabolic and ionic state of the muscle, resulting in a depression of muscle fiber conduction velocity, and subsequently the MPF (Fig. 2*A*). After the rest period of 10 min, the MPF had recovered to prefatigue values. The frequency compression of the power spectrum is primarily governed by shape alterations in the MUAP waveforms that comprise the signal, with minimal influence from MU firing rates (Hermens et al. 1992). The recovery of the MPF thus suggests that the MFCV and hence duration of the MUAP have also been restored to prefatigue values.

The decline in MPF postfatigue was accompanied by a simultaneous rise in sEMG amplitude (Fig. 2*B*). Although the complexity of the surface signal limits the utility of EMG amplitude as an index of muscle activation, an increase during and immediately following sustained submaximal contractions is usually considered to indicate an enhancement of the central drive (Bigland-Ritchie et al. 1986b; Fuglevand et al. 1993a), although it can be influenced by surges in Na^+-K^+-pump activity, MU synchronization and rate coding, and prolonged duration of the underlying MUAP shape due to decreased conduction velocity (Farina et al. 2004; Hicks and McComas 1989; Lowery and O'Malley 2003). This increase in the intensity of the central drive increases the number of MUs recruited and/or modulates the firing rates of previously active MUs (Fuglevand et al. 1993b).

In the present study, a reduction in mean firing rates was observed postfatigue, which suggests that MU rate coding was not a contributing factor to the rise in sEMG amplitude (Gabriel and Kamen 2009). However, the contribution of MU synchronization, which has been proposed to increase following fatigue (Holtermann et al. 2009), in augmenting sEMG amplitude cannot be excluded. After a period of rest, sEMG amplitude remained elevated, disparate from the observed recovery of the signal frequency content. The decoupling of spectral and amplitude properties provides evidence that changes in the muscle fiber action potential waveforms and reduction in conduction velocity are not the primary factor responsible for the enlargement of the EMG signal amplitude.

Changes in MUAP amplitude and duration. Properties of decomposed MUAP waveforms mirrored the changes observed in the global EMG signal (Fig. 8), and a strong correlation was observed between MUAP amplitude and RMS sEMG (Fig. 8*A*) and MUAP duration and sEMG MPF (Fig. 8*B*). The inverse relationship between MUAP duration and MPF has been previously demonstrated in simulation studies (Hermens et al. 1992; Lowery and O'Malley 2003) and investigated using dEMG techniques (Calder et al. 2008). However, the large sample population in this study enabled a significant correlation between the two parameters to be demonstrated experimentally for the first time. MUAP duration increased significantly immediately postfatigue and returned to initial values after a 10-min recovery (Fig. 5*B*). However, MUAP amplitude increased directly following the fatiguing contraction and remained elevated after the rest period (Fig. 5*C*), despite the median MU duration returning to prefatigue levels (Fig. 5*B*). This suggests that the increase in MUAP amplitude observed postrecovery is unlikely to be due to the ionic disturbances that alter MUAP waveforms during fatigue. A more plausible interpretation is that the increase in amplitude is predominantly due to the recruitment of additional large MUs to compensate for the reduction in the force-generating capacity of the muscle (Fig. 6*A*) (Bigland-Ritchie et al. 1986b; Carpentier et al. 2001; Enoka et al. 1989; Maton and Gamet 1989).

A uniform increase in the median and SD of the MUAP durations was observed postfatigue in Fig. 4*B*. If larger MUs, associated with higher conduction velocities and shorter MUAP durations, are recruited to compensate for force loss, a greater range in the population durations may be expected. However, the results of this study support the findings of Gazzoni et al. (2005), who determined that changes in membrane properties due to the activity of recruited muscle fibers influence the conduction velocity of quiescent fibers and newly recruited MUs. Thus an increase in the duration of newly recruited MUAPs with respect to their durations in an unfatigued state would be expected, and is substantiated by the absence of lower range durations postfatigue in this study, despite their presence before fatigue and after recovery.

Lastly, surface-detected action potentials from MUs located at greater depths within the muscle will tend to have larger durations due to the spatial low pass filtering effect of the tissue. The volume conductor effect means that MUAPs of deeper MUs will have longer durations and attenuated amplitudes with respect to more superficial units (Dimitrova and Dimitrov 2003; Lowery et al. 2002). The recruitment of MUs according to spatial distribution, however, is unlikely to bias the overall result of the study, as the FDI muscle has been reported to have a uniform distribution of large and small MUs, with the muscle fibers that comprise each unit widely dispersed (Milner-Brown and Stein 1975).

While the changes in MU duration during fatigue are well established, the variations in MUAP amplitude are less clear. Evidence for peripheral factors inducing changes in MUAP amplitude during fatigue can be found in the literature. A decline in M-wave amplitude has been reported directly after fatiguing contractions when there remained a strong influence of ion channel activity and concentration gradients on the intracellular action potential (Carpentier et al. 2001; Fuglevand et al. 1993a). A full recovery of the M-wave has been demonstrated after a 10-min rest period (Fuglevand and Keen 2003; Post et al. 2008), indicating that the restoration of membrane excitability follows a similar time course. The recovery of MPF (Fig. 2*A*), and action potential duration (Fig. 6*B*), after the rest period in the present study suggest the ionic and metabolic changes are unlikely to have substantially influenced the increased sEMG and MUAP amplitudes following recovery.

Response to the impairment of muscle force-generating capacity. It is not possible to infer from the sEMG and MUAPs parameters whether one single mechanism or a combination of mechanisms is responsible for the decrease of the mechanical muscle force (Allen et al. 2008; Enoka and Duchateau 2008). Prolonged low-frequency force depression and reduced MVC and twitch force following sustained contractions have been previously attributed to excitation-contraction coupling failure in several studies (Hill et al. 2001; Westerblad et al. 1998). The prolonged reduction in the force-generating capacity of the muscle is compensated by the recruitment of larger MUs, as reflected in the increase of the amplitude of the sEMG signal (Fig. 2*C*). A reduction in the threshold of MU activation for previously active MUs may be an additional compensatory strategy employed directly postfatigue, where there is evidence of recruitment compression (Fig. 7). The lowering of MU recruitment threshold may be peripherally mediated by changes in the mechanical and metabolic properties of the muscle and could potentially counteract the decline in force attributable to the reduction in MU firing rates. Despite the absence of recruitment compression postrecovery, the percent increase in the mean amplitude of the MUs recruited at each threshold, averaged over all subjects, remained elevated, particularly at the latter stages of recruitment. This suggests that fatigue-induced lowering of the recruitment threshold of larger MUs was also employed postrecovery to compensate for the continued force impairment of those MUs already activated (Adam and De Luca 2003; Calder et al. 2008; Carpentier et al. 2001; Farina et al. 2009). The slope of the regression fit to the MUAP amplitude and threshold relationship exhibited an overall tendency to increase directly postfatigue, which corresponds with the reported recruitment compression. However, across all subjects there was no systematic change observed in the slope of the regression fit after the recovery period, which implies that the compensatory strategies employed to cope with a force deficit may be specific to the individual. Supplementary MU activation and lower MU recruitment thresholds could both be present in varying combinations after fatigue.

Firing rate and uniformity of changes. The current study offers a more comprehensive insight into firing rate alterations after muscle fatigue than previous reports on pooled single MU observations by simultaneously examining the firing patterns of hundreds of MUs in each condition, across all subjects. In addition, the recording configuration allows the uniformity of MU adaptations to be investigated across a sample population with different thresholds of recruitment. The reduction in the mean MU firing rates observed following fatigue mirrors previous studies reporting an overall decline in MU discharge rates with the development of fatigue (Calder et al. 2008; Christova and Kossev 1998; Stock et al. 2012). Furthermore, average MU firing rates were consistently lower over the range of MU recruitment thresholds (Fig. 6*B*), which suggests that the reported decline was not a simply a consequence of the lower discharge rates of newly recruited MUs. Although previous studies have shown that newly recruited MUs can increase their discharge rate as fatigue progresses (Adam and De Luca 2005; Garland et al. 1994), the results of this study show that over the MU population discharge rates display a uniform reduction in response to fatigue (Fig. 6*B*). The reduction in discharge frequency may occur as a result of a decline in the intrinsic excitability of MUs with previous activity (Kernell and Monster 1982), or alternatively, firing rate may be modulated by inhibitory afferent signals from receptors sensitive either to changes in the muscle contractile properties or to the metabolic state of the muscle (Bigland-Ritchie et al. 1986a). In this study, alterations to MU discharge rates were negatively correlated with changes in MUAP duration, which may imply a role for metabolically activated inhibitory inputs in regulating MU firing. Proprioceptive feedback from muscle spindles (De Luca and Kline 2012) and Golgi tendon organs (Kirsch and Rymer 1987) may also contribute to the control of MU activity, although simultaneous recovery of firing rate and MUAP duration was observed after rest with only partial restoration of force.

There were no consistent trends in the alterations to MU discharge rate or MUAP amplitude or duration to suggest that higher threshold MUs were systematically more affected by fatigue, and results varied by subject. This finding may be due to the low target force of the 20% MVC test contractions sampling a relatively homogeneous group of fatigue-resistant MUs. Alternatively, the longer hold phase of the fatigue task may have resulted in all detected MUs being active for similar durations, thus the activity dependent adjustments would be comparable across the MU pool. Lastly, it is likely that the intensity of the fatigue task induced widespread changes in the conduction velocity of all muscle fibers and was not confined to distinct MU territories.

Conclusion. This study is the first to simultaneously examine global sEMG and the properties of a large population of individual MUAPs, complete with recruitment threshold and firing rate information, before and immediately after a sustained isometric fatiguing contraction, and following a recovery period. Changes in the properties of the recruited MU population were found to be consistent with alterations observed in the global EMG signal and displayed well-established manifestations of fatigue over a large MU population. The observed increase in sEMG and MUAP amplitude postfatigue is consistent with previous studies that have demonstrated MU recruitment during fatiguing contractions using intramuscular, conventional sEMG, and surface decomposition techniques. MUAP duration and MPF were restored to initial prefatigue values following the rest period, suggesting that the fatigue-induced ionic and metabolic alterations that affect MFCV have also recovered. Despite the increase in central drive postfatigue, MU firing rates were reduced, implying that to maintain force during fatigue, recruitment is favored over rate coding while MUs are available. The presence of recruitment compression postfatigue may imply a peripherally mediated lowering of the MU recruitment threshold as an additional short-term compensatory mechanism to cope with large fatigue-induced force deficits. Although recruitment compression was absent after the recovery period, sEMG and MUAP amplitude remained elevated, and additional recruitment was still required to compensate for the continued impairment to the force. MU discharge rates returned to initial values after rest, mirroring the recovery of MFCV. This provides evidence that the changes in MU firing are modulated by inhibitory afferents sensitive to the metabolic state of the muscle. In conclusion, this study employs sEMG decomposition techniques to examine fatigue-induced changes in the properties of a MU population and outlines possible recruitment strat-

egies that may be employed to compensate for force deficits due to both short-term alterations in the metabolic state of the muscle and long-term variations in muscle contractile properties.

GRANTS

Funding for this work was provided by the Irish Research Council.

DISCLOSURES

No conflicts of interest, financial or otherwise, are declared by the author(s).

AUTHOR CONTRIBUTIONS

Author contributions: L.M., M.M.L., and N.L.S. conception and design of research; L.M., X.H., and N.L.S. performed experiments; L.M., X.H., and N.L.S. analyzed data; L.M., W.Z.R., M.M.L., and N.L.S. interpreted results of experiments; L.M. prepared figures; L.M., M.M.L., and N.L.S. drafted manuscript; L.M., W.Z.R., M.M.L., and N.L.S. edited and revised manuscript; L.M., X.H., W.Z.R., M.M.L., and N.L.S. approved final version of manuscript.

REFERENCES

Adam A, De Luca CJ. Firing rates of motor units in human vastus lateralis muscle during fatiguing isometric contractions. *J Appl Physiol* 99: 268–280, 2005.

Adam A, De Luca CJ. Recruitment order of motor units in human vastus lateralis muscle is maintained during fatiguing contractions. *J Neurophysiol* 90: 2919–2927, 2003.

Allen DG, Lamb G, Westerblad H. Skeletal muscle fatigue: cellular mechanisms. *Physiol Rev* 88: 287–332, 2008.

Beck TW, Kasishke PR, Stock MS, DeFreitas JM. Eccentric exercise does not affect common drive in the biceps brachii. *Muscle Nerve* 46: 759–766, 2012.

Bigland-Ritchie B, Dawson N, Johansson R, Lippold O. Reflex origin for the slowing of motoneurone firing rates in fatigue of human voluntary contractions. *J Physiol* 379: 451–459, 1986a.

Bigland-Ritchie B, Furbush F, Woods J. Fatigue of intermittent submaximal voluntary contractions central and peripheral factors. *J Appl Physiol* 61: 421–429, 1986b.

Calder KM, Stashuk DW, McLean L. Physiological characteristics of motor units in the brachioradialis muscle across fatiguing low-level isometric contractions. *J Electromyogr Kinesiol* 18: 2–15, 2008.

Carpentier A, Duchateau J, Hainaut K. Motor unit behaviour and contractile changes during fatigue in the human first dorsal interosseus. *J Physiol* 534: 903–912, 2001.

Christova P, Kossev A. Motor unit activity during long-lasting intermittent muscle contractions in humans. *Eur J Appl Physiol Occup Physiol* 77: 379–387, 1998.

De Luca C, Kline J. Influence of proprioceptive feedback on the firing rate and recruitment of motoneurons. *J Neural Eng* 9: 016007, 2012.

De Luca CJ, Hostage EC. Relationship between firing rate and recruitment threshold of motoneurons in voluntary isometric contractions. *J Neurophysiol* 104: 1034–1046, 2010.

De Luca CJ, Nawab SH. Reply to Farina and Enoka: the reconstruct-and-test approach is the most appropriate validation for surface EMG signal decomposition to date. *J Neurophysiol* 105: 983–984, 2011.

Defreitas JM, Beck TW, Ye X, Stock MS. Synchronization of low- and high-threshold motor units. *Muscle Nerve* 49: 575–583, 2014.

Dimitrova N, Dimitrov G. Interpretation of EMG changes with fatigue: facts, pitfalls, and fallacies. *J Electromyogr Kinesiol* 13: 13–36, 2003.

Dorfman LJ, Howard JE, McGill KC. Triphasic behavioral response of motor units to submaximal fatiguing exercise. *Muscle Nerve* 13: 621–628, 1990.

Enoka RM, Duchateau J. Muscle fatigue: what, why and how it influences muscle function. *J Physiol* 586: 11–23, 2008.

Enoka RM, Robinson GA, Kossev AR. Task and fatigue effects on low-threshold motor units in human hand muscle. *J Neurophysiol* 62: 1344–1359, 1989.

Esposito F, Orizio C, Veicsteinas A. Electromyogram and mechanomyogram changes in fresh and fatigued muscle during sustained contraction in men. *Eur J Appl Physiol Occup Physiol* 78: 494–501, 1998.

Farina D, Holobar A, Gazzoni M, Zazula D, Merletti R, Enoka RM. Adjustments differ among low-threshold motor units during intermittent, isometric contractions. *J Neurophysiol* 101: 350–359, 2009.

Farina D, Merletti R, Enoka RM. The extraction of neural strategies from the surface EMG. *J Appl Physiol* 96: 1486–1495, 2004.

Fuglevand A, Zackowski K, Huey K, Enoka R. Impairment of neuromuscular propagation during human fatiguing contractions at submaximal forces. *J Physiol* 460: 549–572, 1993a.

Fuglevand AJ, Keen DA. Re-evaluation of muscle wisdom in the human adductor pollicis using physiological rates of stimulation. *J Physiol* 549: 865–875, 2003.

Fuglevand AJ, Winter DA, Patla AE. Models of recruitment and rate coding organization in motor-unit pools. *J Neurophysiol* 70: 2470–2488, 1993b.

Gabriel DA, Kamen G. Experimental and modeling investigation of spectral compression of biceps brachii SEMG activity with increasing force levels. *J Electromyogr Kinesiol* 19: 437–448, 2009.

Garland S, Enoka R, Serrano L, Robinson G. Behavior of motor units in human biceps brachii during a submaximal fatiguing contraction. *J Appl Physiol* 76: 2411–2419, 1994.

Gazzoni M, Camelia F, Farina D. Conduction velocity of quiescent muscle fibers decreases during sustained contraction. *J Neurophysiol* 94: 387–394, 2005.

Gazzoni M, Farina D, Merletti R. A new method for the extraction and classification of single motor unit action potentials from surface EMG signals. *J Neurosci Methods* 136: 165–177, 2004.

Hermens H, Bruggen T, Baten C, Rutten W, Boom H. The median frequency of the surface EMG power spectrum in relation to motor unit firing and action potential properties. *J Electromyogr Kinesiol* 2: 15–25, 1992.

Hicks A, McComas A. Increased sodium pump activity following repetitive stimulation of rat soleus muscles. *J Physiol* 414: 337–349, 1989.

Hill CA, Thompson MW, Ruell PA, Thom JM, White MJ. Sarcoplasmic reticulum function and muscle contractile character following fatiguing exercise in humans. *J Physiol* 531: 871–878, 2001.

Hogrel JY. Use of surface EMG for studying motor unit recruitment during isometric linear force ramp. *J Electromyogr Kinesiol* 13: 417–423, 2003.

Holobar A, Farina D, Gazzoni M, Merletti R, Zazula D. Estimating motor unit discharge patterns from high-density surface electromyogram. *Clin Neurophysiol* 120: 551–562, 2009.

Holtermann A, Grönlund C, Karlsson JS, Roeleveld K. Motor unit synchronization during fatigue: described with a novel sEMG method based on large motor unit samples. *J Electromyogr Kinesiol* 19: 232–241, 2009.

Hu X, Rymer WZ, Suresh NL. Accuracy assessment of a surface electromyogram decomposition system in human first dorsal interosseus muscle. *J Neural Eng* 11: 026007, 2014.

Hu X, Rymer WZ, Suresh NL. Assessment of validity of a high-yield surface electromyogram decomposition. *J Neuroeng Rehab* 10: 99, 2013a.

Hu X, Rymer WZ, Suresh NL. Reliability of spike triggered averaging of the surface electromyogram for motor unit action potential estimation. *Muscle Nerve* 48: 557–570, 2013b.

Hu X, Suresh AK, Li X, Rymer WZ, Suresh NL. Impaired motor unit control in paretic muscle post stroke assessed using surface electromyography: a preliminary report. In: *Engineering in Medicine and Biology Society (EMBC), 2012 Annual International Conference of the IEEE*. San Diego, CA: IEEE, 2012, p. 4116–4119.

Jensen B, Pilegaard M, Sjøgaard G. Motor unit recruitment and rate coding in response to fatiguing shoulder abductions and subsequent recovery. *Eur J Appl Physiol* 83: 190–199, 2000.

Kallenberg LA, Hermens HJ. Behaviour of a surface EMG based measure for motor control: motor unit action potential rate in relation to force and muscle fatigue. *J Electromyogr Kinesiol* 18: 780–788, 2008.

Kernell D, Monster A. Time course and properties of late adaptation in spinal motoneurones of the cat. *Exp Brain Res* 46: 191–196, 1982.

Kirsch R, Rymer W. Neural compensation for muscular fatigue: evidence for significant force regulation in man. *J Neurophysiol* 57: 1893–1910, 1987.

Kleine BU, van Dijk JP, Zwarts MJ, Stegeman DF. Inter-operator agreement in decomposition of motor unit firings from high-density surface EMG. *J Electromyogr Kinesiol* 18: 652–661, 2008.

Lowery MM, Nolan P, O'Malley MJ. Electromyogram median frequency, spectral compression and muscle fibre conduction velocity during sustained sub-maximal contraction of the brachioradialis muscle. *J Electromyogr Kinesiol* 12: 111–118, 2002.

Lowery MM, O'Malley MJ. Analysis and simulation of changes in EMG amplitude during high-level fatiguing contractions. *IEEE Trans Biomed Eng* 50: 1052–1062, 2003.

Maton B, Gamet D. The fatigability of two agonistic muscles in human isometric voluntary submaximal contraction: an EMG study. *Eur J Appl Physiol Occup Physiol* 58: 369–374, 1989.

Milner-Brown H, Stein R. The relation between the surface electromyogram and muscular force. *J Physiol* 246: 549–569, 1975.

Nawab SH, Chang SS, De Luca CJ. High-yield decomposition of surface EMG signals. *Clin Neurophysiol* 121: 1602–1615, 2010.

Post M, Bayrak S, Kernell D, Zijdewind I. Contralateral muscle activity and fatigue in the human first dorsal interosseous muscle. *J Appl Physiol* 105: 70–82, 2008.

Stock MS, Beck TW, Defreitas JM. Effects of fatigue on motor unit firing rate versus recruitment threshold relationships. *Muscle Nerve* 45: 100–109, 2012.

Suresh N, Kuo A, Heckman C, Ellis M, Rymer W. Correlation of mechanical action with directional tuning in the first dorsal interosseous (FDI). In: *Proceedings of the XIVth Congress of the International Society for Electrophysiology and Kinesiology*. Vienna, Austria: International Society for Electrophysiology and Kinesiology, 2002.

Thomas CK, Johansson RS, Bigland-Ritchie B. EMG changes in human thenar motor units with force potentiation and fatigue. *J Neurophysiol* 95: 1518–1526, 2006.

Westerblad H, Allen D, Bruton J, Andrade F, Lännergren J. Mechanisms underlying the reduction of isometric force in skeletal muscle fatigue. *Acta Physiol Scand* 162: 253–260, 1998.